Inorganic Chemistry
Article

Inorg. Chem. **2010**, *49*, 3025–3028 **3025**
DOI: 10.1021/ic902568v

On the Importance of the Interplaquette Spin Exchanges in Na_3RuO_4: Density Functional Theory Analysis of the Spin Exchange and Magnetic Properties

Fang Wu,[†,‡] Erjun Kan,[‡] and Myung-Hwan Whangbo*[,‡]

[†]*School of Science, Nanjing Forestry University, Nanjing, Jiangsu 210037, China, and*
[‡]*Department of Chemistry, North Carolina State University, Raleigh, North Carolina 27695-8204*

Received December 23, 2009

Na_3RuO_4 contains layers of high-spin Ru^{5+} d^3 ions grouped into isolated four-membered plaquettes. To determine the spin−lattice appropriate for Na_3RuO_4, we evaluated the intraplaquette exchanges J_1, J_2, and J_3 as well as the interplaquette exchanges J_4 and J_5 by performing mapping analysis based on first-principles density functional theory calculations. In addition, we examined how the trends in the calculated J_1-J_5 are related to the distortions of the RuO_6 octahedra in the four-membered plaquettes. The spin−lattice of Na_3RuO_4 is described by the intraplaquette exchanges J_1 and J_2 plus the interplaquette exchanges J_4 and J_5, with spin frustration arising from the (J_1, J_2, J_1) and (J_5, J_4, J_5) triangles. The trends in the calculated J_1-J_5 reflect the distortions of the RuO_6 octahedra in the four-membered plaquettes.

1. Introduction

The magnetic oxide Na_3RuO_4[1] has layers of tetramer clusters $(RuO_4)_4$ made up of four edge-sharing RuO_6 octahedra (Figure 1a), which alternate with layers of Na^+ ions (Figure 1b). The Ru atoms of Na_3RuO_4 exist as high-spin Ru^{5+} d^3 ($S = {}^3/_2$) ions,[2−5] and each layer of the Ru^{5+} ions is composed of isolated four-membered plaquettes of Ru^{5+} ions (Figure 1c). According to ^{99}Ru Mössbauer spectroscopy,[3] magnetic susceptibility[4,5] and neutron diffraction[4] studies, Na_3RuO_4 undergoes antiferromagnetic (AFM) three-dimensional order below ∼30 K (i.e., $T_N \approx 30$ K). The Curie−Weiss temperatures θ of Na_3RuO_4, reported to be −141 K[4] and −162 K,[5] show that dominant AFM interactions exist. Because T_N is considerably smaller than $|\theta|$ (i.e., $|\theta|/T_N \approx 5$), substantial geometric spin frustration[6,7] should be present in Na_3RuO_4. The spacing between adjacent layers of the four-membered plaquettes is large, so the interplaquette exchanges between adjacent layers would be weak compared with those within each layer. As for the intralayer exchanges, one might consider the three intraplaquette exchanges J_1-J_3 as well as the two interplaquette exchanges J_4 and J_5 (Figure 1c). So far, the magnetic properties of Na_3RuO_4 have been discussed solely on the basis of the intraplaquette exchanges. The analysis of the magnetic susceptibility of Na_3RuO_4 in terms of J_1 and J_2 showed that both are AFM with $J_2/J_1 \approx 1.2$,[2] indicating the presence of spin frustration. In the recent neutron scattering study by Haraldsen et al.,[5] the spin-wave dispersion relations were analyzed in terms of the lozenge model (J_1), the double-dimer model (J_2 and J_3), and the coupled-dimer model (J_1, J_2, J_3). They found that Na_3RuO_4 is not describable as a spin-lozenge or other finite tetramer model, hence suggesting the need to take into consideration the intercluster spin exchanges J_4 and J_5.

The magnetic properties of a given magnetic solid are described in terms of a chosen spin−lattice and the associated spin Hamiltonian. It is necessary that a chosen spin−lattice be consistent with the electronic structure of the magnetic system because it is the latter that determines the magnetic energy spectrum.[8,9] Experimentally, the spin-exchange parameters of a chosen spin−lattice are determined as the fitting parameters that best simulate the experimental data (e.g., the spin-wave dispersion relations from inelastic neutron scattering, the temperature dependence of the magnetic susceptibility, and that of the specific heat). Unfortunately, the correctness of a chosen spin−lattice is not necessarily

*To whom correspondence should be addressed. E-mail: mike_whangbo@ncsu.edu.

(1) Darriet, J.; Galy, J. *Bull. Soc. Fr. Minér. Cristallogr.* **1974**, *97*, 3.
(2) Drillon, M.; Darriet, J.; Georges, R. *J. Phys. Chem. Solids* **1977**, *38*, 411.
(3) Gibb, T. C.; Greatrex, R.; Greenwood, N. N. *J. Solid State Chem.* **1980**, *31*, 153.
(4) Regan, K. A.; Huang, Q.; Cava, R. J. *J. Solid State Chem.* **2005**, *178*, 2104.
(5) Haraldsen, J. T.; Stone, M. B.; Lumsden, M. D.; Barnes, T.; Jin, R.; Taylor, J. W.; Fernandez-Alonso, F. *J. Phys.: Condens. Matter* **2009**, *21*, 506003.
(6) Greedan, J. E. *J. Mater. Chem.* **2001**, *11*, 37 and references cited therein.
(7) Dai, D.; Whangbo, M.-H. *J. Chem. Phys.* **2004**, *121*, 672.
(8) Illas, F.; de P. R. Moreira, I.; de Graaf, C.; Varone, D. *Theor. Chem. Acc.* **2000**, *104*, 265.
(9) (a) Whangbo, M.-H.; Koo, H.-J.; Dai, D. *J. Solid State Chem.* **2003**, *176*, 417. (b) Whangbo, M.-H.; Dai, D.; Koo, H.-J. *Solid State Sci.* **2005**, *7*, 827.

Published on Web 02/10/2010

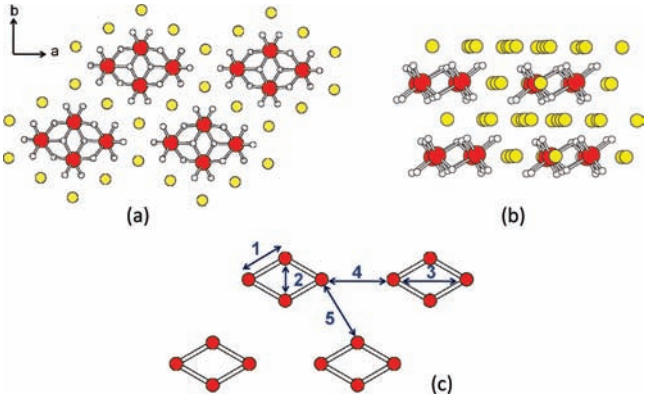

Figure 1. Structural features of Na_3RuO_4: (a) Projection view of a layer of tetramer clusters $(RuO_4)_4$ surrounded by Na^+ ions, where the red white, and yellow circles represent the Ru, O, and Na atoms, respectively. (b) Side view of the layers of tetramer clusters $(RuO_4)_4$ alternating with layers of Na^+ ions. (c) Projection view of a layer of Ru^{5+} ions, which appear as four-membered plaquettes. The numbers 1−5 represent the spin exchanges J_1−J_5, respectively.

guaranteed even if it provides an excellent fitting as found for $(VO)_2P_2O_7$,[10,11] $Na_3Cu_2SbO_6$ and $Na_2Cu_2TeO_6$,[12−16] $Bi_4Cu_3V_2O_{14}$,[17−20] and $Cu_3(CO_3)_2(OH)_2$,[21,22] to name a few. In identifying the correct spin−lattice of a magnetic system, electronic structure calculations are indispensable.

In Na_3RuO_4, the intraplaquette spin exchanges J_1 and J_2 are of the superexchange (SE) type involving Ru−O−Ru paths, while the intraplaquette exchange J_3 as well as the interplaquette exchanges J_4 and J_5 are of the supersuperexchange (SSE) type involving Ru−O···O−Ru paths.[9] Recent studies on numerous magnetic oxides have shown that SSE interactions can be much stronger than SE interactions, although they are frequently neglected without justifiable reasons.[9,11,15,20,22] To determine the spin−lattice appropriate for Na_3RuO_4, it is necessary to evaluate the relative strengths of the spin exchanges J_1−J_5. In the present work, we determine the values of J_1−J_5 by performing mapping analysis based on first-principles density functional theory (DFT) calculations.[9,11,15,20,22] To account for the trends in the calculated J_1−J_5 values, we then probe how they are related to the distortions of the RuO_6 octahedra in the tetramer clusters (Figure 1a).

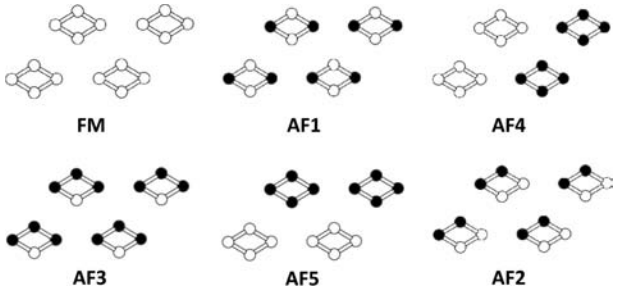

Figure 2. Six ordered spin states of Na_3RuO_4 employed to extract the spin exchanges J_1−J_5 by mapping analysis based on DFT calculations, where the unshaded and shaded circles represent the Ru^{5+} ions with up-spin and down-spin, respectively.

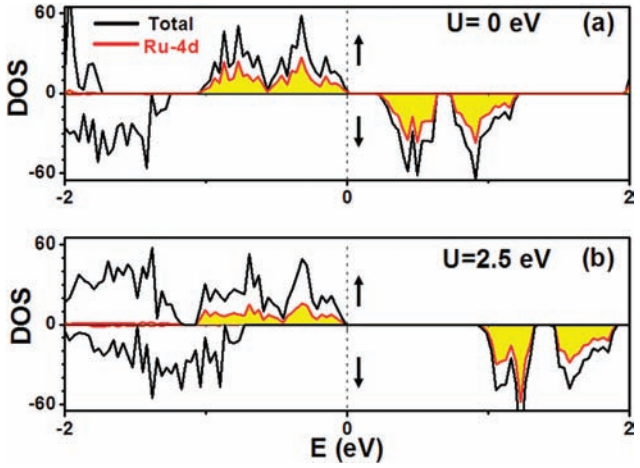

Figure 3. Plots of the total DOS and PDOS for the Ru 4d states obtained for the FM state of Na_3RuO_4 (a) from the GGA calculations and (b) from the GGA+U calculations with U = 2.5 eV on Ru.

Table 1. Relative Energies (in meV) of the Six Ordered Spin States Obtained from GGA+U Calculations

U (eV)	FM	AF1	AF2	AF3	AF4	AF5
0.0	0	−50.7	−43.0	−32.3	−22.1	−22.0
2.5	0	−21.1	−18.0	−12.1	−12.1	−12.2
4.0	0	−13.6	−11.4	−7.1	−8.9	−9.0

2. Evaluation of Spin-Exchange Parameters

To extract the values of J_1−J_5 on the basis of DFT calculations, we first calculate the total energies of the six ordered spin states of Na_3RuO_4 depicted in Figure 2. Our spin-polarized DFT calculations employed the projector augmented wave method implemented in the *Vienna* ab initio simulation package[23] with the generalized gradient approximation (GGA)[24] for the exchange-correlation functional, the plane-wave cutoff energy 400 eV, a set of $2 \times 2 \times 7$ k points,[25] and the threshold 10^{-5} eV for energy convergence. Figure 3a shows plots of the total density of states (DOS) and

(10) Garret, A. W.; Nagler, S. E.; Tennant, D. A.; Sales, B. C.; Barnes, T. *Phys. Rev. Lett.* **1997**, *79*, 745.
(11) Koo, H.-J.; Whangbo, M.-H.; VerNooy, P. D.; Torardi, C. C.; Marshall, W. J. *Inorg. Chem.* **2002**, *41*, 4664.
(12) Xu, J.; Assoud, A.; Soheilnia, N.; Derakhshan, S.; Cuthbert, H. L.; Greedan, J. E.; Whangbo, M.-H.; Kleinke, H. *Inorg. Chem.* **2005**, *44*, 5042.
(13) Miura., Y.; Hirai, R.; Kobayashi, Y.; Sato, M. *J. Phys. Soc. Jpn.* **2006**, *75*, 84707.
(14) Derakhshan, S.; Cuthbert, H. L.; Greedan, J. E.; Rahman, B.; Saha-Dasgupta, T. *Phys. Rev. B* **2007**, *76*, 104403.
(15) Koo, H.-J.; Whangbo, M.-H. *Inorg. Chem.* **2008**, *47*, 128.
(16) Miura, Y.; Yasui, Y.; Moyoshi, T.; Sato, M.; Kakurai, K. *J. Phys. Soc. Jpn.* **2008**, *77*, 104789.
(17) Sakurai, H.; Yoshimura, K.; Kosuge, K.; Tsujii, N.; Abe, H.; Kitazawa, H.; Kido, G.; Michor, H.; Hilscher, G. *J. Phys. Soc. Jpn.* **2002**, *71*, 1161.
(18) Okubo, S.; Hirano, T.; Inagaki, Y.; Ohta, H.; Sakurai, H.; Yoshimura, H.; Kosuge, K. *Physica B* **2004**, *346*, 65.
(19) Okamoto, K.; Tonegawa, T.; Kaburagi, M. *J. Phys.: Condens. Matter* **2003**, *15*, 5979.
(20) Koo, H.-J.; Whangbo, M.-H. *Inorg. Chem.* **2008**, *47*, 4779.
(21) Rule, K. C.; Wolter, A. U. B.; Süllow, S.; Tennant, D. A.; Brühl, A.; Köhler, S.; Wolf, B.; Lang, M.; Schreuer, J. *Phys. Rev. Lett.* **2008**, *100*, 117202.
(22) Kang, J.; Lee, C.; Kremer, R. K.; Whangbo, M.-H. *J. Phys.: Condens. Matter* **2009**, *21*, 392201.
(23) (a) Kresse, G.; Hafner, J. *Phys. Rev. B* **1993**, *62*, 558. (b) Kresse, G.; Furthmüller, J. *Comput. Mater. Sci.* **1996**, *6*, 15. (c) Kresse, G.; Furthmüller, J. *Phys. Rev. B* **1996**, *54*, 11169.
(24) Perdew, J. P.; Burke, S.; Ernzerhof, M. *Phys. Rev. Lett.* **1996**, *77*, 3865.
(25) Dudarev, S. L.; Botton, G. A.; Savrasov, S. Y.; Humphreys, C. J.; Sutton, A. P. *Phys. Rev. B* **1998**, *57*, 1505.

Table 2. Spin-Exchange Parameters J_1−J_5 (in meV) Obtained from GGA+U Calculations[a]

U (eV)	J_1	J_2	J_3	J_4	J_5
0.0	−6.38 (0.69)	−6.18 (0.67)	0.36 (−0.04)	−9.18 (1.00)	−4.90 (0.53)
2.5	−1.99 (0.37)	−1.36 (0.25)	0.10 (−0.02)	−5.34 (1.00)	−2.71 (0.51)
4.0	−1.02 (0.26)	−0.55 (0.14)	0.07 (−0.02)	−3.91 (1.00)	−1.99 (0.51)

[a] The numbers in parentheses are relative values.

the projected DOS (PDOS) for the Ru 4d states, obtained from GGA calculations for the ferromagnetic (FM) state of Na_3RuO_4. All up-spin t_{2g} states are occupied and are separated with a band gap from the down-spin t_{2g} states lying above. This is consistent with the finding that Na_3RuO_4 consists of high-spin Ru^{5+} d^3 ions and is a magnetic insulator.

In general, the electron correlation associated with 3d states is not well-described by DFT calculations, and this deficiency is commonly corrected by using the GGA plus on-site repulsion U (GGA+U) method.[25] The electron correlation in Na_3RuO_4 may not be strong because 4d states are generally less contracted than 3d states. Nevertheless, to see the possible effects of electron correlation, we also carried out GGA+U calculations with U = 2.5 and 4.0 eV. Figure 3b shows plots of the total DOS and PDOS for the Ru 4d states, obtained from GGA+U calculations (with U = 2.5 eV) for the FM state of Na_3RuO_4. Concerning the presence of high-spin Ru^{5+} ions and an insulating band gap in Na_3RuO_4, both GGA and GGA+U calculations present the same picture. As expected, the band gap is predicted to be greater by the GGA+U calculations than by the GGA calculations. The relative energies of the six ordered spin states of Na_3RuO_4 (Figure 2), obtained from our GGA+U (with U = 0.0, 2.5, and 4.0 eV), are summarized in Table 1.

To determine the values of J_1−J_5, we express the energies of the six ordered spin states in terms of the spin Hamiltonian:

$$\hat{H} = -\sum_{i<j} J_{ij}\hat{S}_i \cdot \hat{S}_j \qquad (1)$$

in which J_{ij} (=J_1−J_5) is the exchange parameter for the interaction between the spin sites i and j, while $\hat{S}_i$ and $\hat{S}_j$ are the spin angular momentum operators at the spin sites i and j, respectively. When the energy expressions obtained for spin dimers with N unpaired spins per spin site are applied (in the present case, N = 3),[26] the total spin-exchange energies (per formula unit) of the six ordered spin states are written as

$$\begin{aligned} E_{FM} &= (-4J_1 - J_2 - J_3 - J_4 - 4J_5)N^2/16 \\ E_{AF1} &= (+4J_1 - J_2 - J_3 - J_4 + 4J_5)N^2/16 \\ E_{AF2} &= (+J_2 + J_3 + J_4)N^2/16 \\ E_{AF3} &= (+J_2 - J_3 - J_4)N^2/16 \\ E_{AF4} &= (-4J_1 - J_2 - J_3 + J_4)N^2/16 \\ E_{AF5} &= (-4J_1 - J_2 - J_3 - J_4 + 4J_5)N^2/16 \qquad (2) \end{aligned}$$

Therefore, the values of J_1−J_5 listed in Table 2 are determined by equating the relative energies of the six ordered spin states obtained from GGA+U calculations to the corresponding relative energies obtained from the total spin-exchange energies.

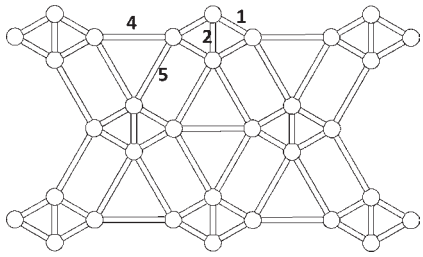

Figure 4. Spin−lattice of Na_3RuO_4 predicted from the intraplaquette exchanges J_1 and J_2 as well as the interplaquette exchanges J_4 and J_5. The numbers 1, 2, 4, and 5 represent J_1, J_2, J_4, and J_5, respectively.

From the spin-exchange values of Table 2, the following are observed:

(a) In the GGA and GGA+U calculations, the strongest AFM exchange is the interplaquette exchange J_4, and the intraplaquette exchange J_3 is negligibly weak.

(b) In the GGA calculations, the interplaquette AFM exchange J_5 is comparable in strength to the intraplaquette AFM exchanges J_1 and J_2. The AFM exchanges J_1, J_2, J_4, and J_5 give rise to the spin−lattice presented in Figure 4, where the (J_1, J_5, J_1, J_5) rectangles lead to AFM order, while the (J_1, J_2, J_1) and (J_5, J_4, J_5) triangles lead to spin frustration. The latter agrees well with the experimental fact that T_N is considerably smaller than $|\theta|$.[6,7] It is possible that the spins of Na_3RuO_4 may adopt a noncollinear structure to reduce the extent of spin frustration. To confirm this prediction, neutron diffraction on single-crystal samples is necessary.

(c) Comparison of the GGA and GGA+U calculations shows that the magnitudes of the AFM exchanges decrease with increasing on-site repulsion U on Ru; the intraplaquette exchanges J_1 and J_2 decrease faster than do the interplaquette exchanges J_4 and J_5. Thus, when U increases, the interplaquette exchanges J_4 and J_5 become more important than the intraplaquette exchanges J_1 and J_2. However, the J_5/J_4 ratio (i.e., ∼0.5) does not depend on U.

(d) Although J_4 is the strongest AFM interaction, the most stable one among the six ordered spin states is AF1, in which the spins of the J_4 paths are ferromagnetically coupled. This is due to the fact that, per Ru_4 plaquette, there occur four J_1 and four J_5 interactions, while there occurs only one J_4 interaction.

3. Distortions of the RuO_6 Octahedra and Spin Exchanges

Let us now discuss how the calculated spin-exchange parameters J_1−J_5 are related to the structural parameters associated with their exchange paths. As shown in Figure 5, the $Ru1O_6$ and $Ru2O_6$ octahedra in each tetramer cluster $(RuO_4)_4$ are strongly distorted. The nature of the distortions is readily explained by recognizing the fact that, because of the Coulombic repulsion between the four Ru^{5+} ions, they

(26) (a) Dai, D.; Whangbo, M.-H. *J. Chem. Phys.* **2001**, *114*, 2887. (b) Dai, D.; Whangbo, M.-H. *J. Chem. Phys.* **2003**, *118*, 29.

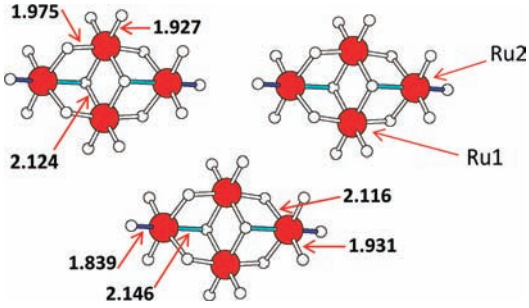

Figure 5. Lengths of the Ru−O bonds (in Å) in the $Ru1O_6$ and $Ru2O_6$ octahedra in the tetramer clusters $(RuO_4)_4$ of Na_3RuO_4, where the shortest and longest Ru2−O bonds are indicated by the blue and cyan cylinders, respectively.

Table 3. Geometrical Parameters Associated with the Spin-Exchange Paths J_1−J_5[a]

(a) SE Paths

	Ru···Ru	Ru−O−Ru	∠Ru−O−Ru
J_1	3.210	2.116, 1.975	103.3
		2.146, 2.124	97.5
J_2	3.210	2.124, 2.124	98.2
		2.124, 2.124	98.2

(b) SSE Paths

	Ru···Ru	Ru−O···O−Ru	∠Ru−O···O, ∠O···O−Ru
J_3	5.559	2.146, 2.782, 2.146	102.2, 102.2
J_4	5.477	1.839, 3.354, 1.931	101.5, 101.5
J_5	7.174	1.839, 3.607, 1.927	147.7, 148.0

[a] The lengths are in angstroms and the angles in degrees.

are displaced away from each other. Consequently, the three Ru2−O bonds away from the cluster center become shorter than those facing the cluster center. Similarly, the two Ru1−O bonds away from the cluster center are shorter than those facing the cluster center.

The local octahedral distortions noted above have important consequences on the nature and strength of the spin exchanges. As listed in Table 3a, the ∠Ru−O−Ru angles of the SE paths J_1 and J_2 are considerably greater than 90°, so it is not surprising that both exchanges are AFM.[27] In general, the strength of an SSE interaction M−O···O−M, where M is a magnetic transition-metal ion, is expected to become strong when the O···O contact distance is short.[9] Table 3a shows that the intraplaquette exchange J_3 has a much shorter O···O contact than does the interplaquette exchange J_4 (2.782 vs 3.354 Å). Nevertheless, J_3 is negligible, but J_4 is strong. To explain this apparently surprising result, we determine the magnetic orbitals of the $Ru1O_6$ and $Ru2O_6$ octahedra by extended Hückel tight-binding calculations.[28] As presented in Figure 6a, the magnetic orbitals of the $Ru2O_6$ octahedron are given by the t_{2g}-block orbitals, in which the Ru 4d and the O 2p orbitals make π-antibonding interactions such that the O 2p contribution is stronger in the shorter Ru−O bond. (Though not shown, the same is true for the

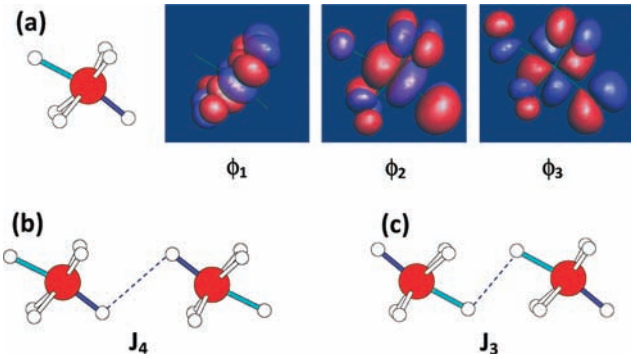

Figure 6. (a) Shapes of the three magnetic orbitals (i.e., the t_{2g} orbitals) of the $Ru2O_6$ octahedron obtained from extended Hückel tight-binding calculations. (b) Arrangement of two $Ru2O_6$ octahedra in the interplaquette spin exchange J_4, in which the two octahedra face each other such that the short Ru2−O bonds of one octahedron make O···O contacts with those of the other octahedron. Only the shortest O···O contact is indicated by the dashed line for simplicity. (c) Arrangement of two $Ru2O_6$ octahedra in the intraplaquette spin exchange J_3, in which the two octahedra face each other such that the long Ru2−O bonds of one octahedron make O···O contacts with those of the other octahedron. Only the shortest O···O contact is indicated by the dashed line for simplicity.

magnetic orbitals of the $Ru1O_6$ octahedron). As a consequence, both O atoms of the SSE path Ru2−O···O−Ru2 have large O 2p orbital contributions in the interplaquette exchange J_4 (Figure 6b) but small O 2p orbital contributions in the intraplaquette exchange J_3 (Figure 6c). This explains why J_3 is negligible despite the short O···O contact of its SSE path Ru−O···O−Ru. It is noted from Figure 5 and Table 3b that the SSE path Ru1−O···O−Ru2 of the interplaquette exchange J_5 involves the shortest Ru1−O and second-shortest Ru2−O bonds, and its O···O contact is slightly longer than that found for J_4 (i.e., 3.607 vs 3.354 Å). This accounts for why J_4 is considerably stronger than J_5.

4. Concluding Remarks

The spin exchanges J_1−J_5 of Na_3RuO_4 extracted from our calculations reveal that J_3 is negligible, and the remaining four spin exchanges are all AFM. The strongest exchange is the interplaquette exchange J_4, and the interplaquette exchange J_5 is comparable in strength to the intraplaquette exchanges J_1 and J_2. The strengths of J_1 and J_2 relative to that of J_5 depend somewhat on U in the GGA+U calculations. However, both our GGA and GGA+U calculations show that Na_3RuO_4 should be described by the intraplaquette exchanges J_1 and J_2 plus the interplaquette exchanges J_4 and J_5, so the (J_1, J_2, J_1) and (J_5, J_4, J_5) triangles of the resulting spin−lattice (Figure 4) give rise to spin frustration. Therefore, our study supports the conclusion by Haraldsen et al.[5] that Na_3RuO_4 is not describable as a spin-lozenge or other finite tetramer model. The observed trends in the spin exchanges J_1−J_5 are intimately related to the distortions of the $Ru1O_6$ and $Ru2O_6$ octahedra in the tetramer clusters $(RuO_4)_4$. To fully test the magnetic structure of Na_3RuO_4 predicted from our theoretical study, it is desirable to carry out experimental studies on single-crystal samples.

Acknowledgment. This work was supported by the Office of Basic Energy Sciences, Division of Materials Sciences, U.S. Department of Energy, under Grant DE-FG02-86ER45259, and also by the computing resources of the NERSC center and the HPC center of NCSU.

(27) Goodenough, J. B. *Magnetism and Chemical Bond*; Wiley: Cambridge, MA, 1963.

(28) (a) Hoffmann, R. *J. Chem. Phys.* **1963**, *39*, 1397. (b) Our calculations were carried out by employing the SAMOA (Structure and Molecular Orbital Analyzer) program package (this program can be downloaded free of charge from the website http://chvamw.chem.ncsu.edu/).